STABILITY OF HIGH ORDER FINITE DIFFERENCE SCHEMES WITH IMPLICIT-EXPLICIT TIME-MARCHING FOR CONVECTION-DIFFUSION AND CONVECTION-DISPERSION EQUATIONS

MEIQI TAN, JUAN CHENG*, AND CHI-WANG SHU

Abstract. The main purpose of this paper is to analyze the stability of the implicit-explicit (IMEX) time-marching methods coupled with high order finite difference spatial discretization for solving the linear convection-diffusion and convection-dispersion equations in one dimension. Both Runge-Kutta and multistep IMEX methods are considered. Stability analysis is performed on the above mentioned schemes with uniform meshes and periodic boundary condition by the aid of the Fourier method. For the convection-diffusion equations, the result shows that the high order IMEX finite difference schemes are subject to the time step restriction $\Delta t \leq \max\{\tau_0, c\Delta x\}$, where τ_0 is a positive constant proportional to the diffusion coefficient and c is the Courant number. For the convection-dispersion equations, we show that the IMEX finite difference schemes are stable under the standard CFL condition $\Delta t \leq c\Delta x$. Numerical experiments are also given to verify the main results.

Key words. Convection-diffusion equation, convection-dispersion equation, stability, IMEX, finite difference, Fourier method.

1. Introduction

In this paper, the stability property of the high order finite difference schemes with certain implicit-explicit (IMEX) time-marching methods is studied for the convection-diffusion and convection-dispersion equations respectively. For the spatial derivative terms of these equations, we use a high order upwind biased finite difference scheme, which is a prototype of the weighted essentially non-oscillatory (WENO) schemes [12, 14], to discretize the convection term, a high order central difference method to discretize the diffusion term, and a high order upwind biased finite difference scheme to discretize the dispersion term.

The time derivative term for the convection-diffusion and convection-dispersion equations should be discretized carefully. If explicit time-marching methods are used, then the time step is dominated by the highest order derivative term, which may be very small, resulting in excessive computational cost. For example, for the convection-dispersion equations involving third order spatial derivatives which are not convection-dominated, the explicit time discretization may suffer from a strict time step restriction $\Delta t \sim O(\Delta x^3)$ for stability, where Δt is the time step and Δx is the spatial mesh size. If the fully implicit time-marching methods are used, then the time step restriction may be relaxed, and usually unconditionally stable such as A-stable schemes can be designed. However, in many practical applications the lower order convection terms are often nonlinear, hence the implicit methods may be much more expensive per time step than the explicit methods, because an iterative solution of the nonlinear algebraic equations is needed.

When it comes to such problems, a natural consideration is to treat different derivative terms differently, that is, the higher order derivative terms are treated implicitly, whereas the rest of the terms are treated explicitly. The IMEX time-marching methods, which have been proposed and studied by many authors [1–7, 9, 10, 13, 16, 17], have considered such a strategy. This can not only alleviate the stringent time step restriction, but also reduce the difficulty of solving the algebraic equations, especially when the higher order derivative terms are linear. Even when the higher order derivative terms are nonlinear, the IMEX time-marching methods might still show their advantages in obtaining a better algebraic system, for example for diffusive higher order derivatives the algebraic system might have some symmetry and positive definite properties, which can be easily solved by many iterative methods.

For the convection-diffusion equations, there have been many studies in the literature on the IMEX methods. In [1], a pair of multistep IMEX time-marching methods are constructed. Coupled with the traditional second order central difference method, the multistep IMEX finite difference schemes are shown to be stable under the standard CFL condition $\Delta t \leq c\Delta x$, where c is the Courant number. However, most of them tend to have an undesirably small c, unless diffusion strongly dominates and an appropriate backward differentiation formula is selected for the diffusion term. In [9], the authors designed several stable multistep IMEX time discretizations, which are specially tailored for stability when coupled with the pseudospectral method. These schemes are shown to be stable provided that the time step and the spatial mesh size are bounded by two constants. Combined with the local discontinuous Galerkin (LDG) method, a variety of IMEX schemes [16,17], including Runge-Kutta type and multistep type IMEX schemes, have been discussed. These schemes are stable provided that the time step is upper-bounded by a positive constant τ_0 which is proportional to d/ν^2, where ν and d are the convection and diffusion coefficients, respectively. However, when d is very small in comparison with the spatial mesh size, τ_0 is too small to be the true bound for stability. For the above mentioned equations without the diffusion terms, the explicit scheme is usually stable under the standard CFL condition. We could therefore reasonably expect that the IMEX method for this convection-diffusion equation should also be stable under the same CFL condition. The schemes in [18], where the explicit part is treated by a strong-stability-preserving Runge-Kutta method [8], and the implicit part is treated by an L-stable diagonally implicit Runge-Kutta method, are also subject to the time step restriction $\Delta t \leq \tau_0$. They also face the problem that τ_0 is too small to be the true bound for stability when d is very small in comparison with the spatial mesh size.

For the convection-dispersion equations, there are also some studies in the literature on the IMEX methods. In [6], some multistep IMEX time-marching methods with the spectral spatial discretization for the KdV equation have been presented. Coupled with the finite volume spatial discretization, some IMEX Runge-Kutta methods are tested in the case of the KdV equation in [5]. These schemes are shown to be stable under the standard CFL condition $\Delta t \leq c\Delta x$. In [10], the IMEX method with the discontinuous Galerkin (DG) spatial discretization is proposed for the KdV equation, where the stability analysis is not discussed.

If we summarize the stability conditions of the schemes mentioned above, we could find that the explicit, implicit and IMEX schemes coupled with appropriate spatial discretizations are subject to the time step restrictions shown in Table 1. Notice that the specific choices of spatial discretizations may change the values of

TABLE 1. The time step restriction for the explicit, implicit and IMEX schemes.

equation	explicit	implicit (A-stable)	IMEX
convection-diffusion	$\Delta t \leq c\Delta x^2$	unconditionally stable	$\Delta t \leq \tau_0$ (constant) or $\Delta t \leq c\Delta x$
convection-dispersion	$\Delta t \leq c\Delta x^3$	unconditionally stable	$\Delta t \leq c\Delta x$

c and τ_0, but not the generic types of stability conditions listed in this table.

In this paper, we will consider certain IMEX finite difference schemes for the convection-diffusion and convection-dispersion equations. For the spatial discretization, we use a high order upwind biased finite difference scheme for the convection term, a high order central difference method for the diffusion term, and a high order upwind biased finite difference scheme for the dispersion term. For simplicity, the stability analysis is performed on the linear equations with the periodic boundary condition using the Fourier method. The following results will be obtained.

1. For the convection-diffusion equations, we obtain two stable third order IMEX finite difference schemes, including Runge-Kutta type and multistep type IMEX schemes, which are subject to the time step restriction $\Delta t \leq \max\{\tau_0, c\Delta x\}$, where τ_0 is a positive constant proportional to the diffusion coefficient and c is the Courant number;

2. For the convection-dispersion equations, we obtain two stable third order IMEX Runge-Kutta finite difference schemes and a second order multistep IMEX finite difference scheme, which are subject to the time step restriction $\Delta t \leq c\Delta x$, where c is the Courant number.

Although the stability analysis is performed on linear equations, the schemes are also applicable to nonlinear equations which will be demonstrated by numerical tests.

The organization of this paper is as follows. In Section 2, we will present two IMEX finite difference schemes for the linear convection-diffusion equation, and will concentrate on the stability analysis of the corresponding schemes. Numerical experiments are also given to demonstrate the stability results given by our analysis. In Section 3, we will provide several numerical examples, including linear and nonlinear equations, to numerically validate the stability condition and the error accuracy for the schemes. Section 4 is similar to Section 2, and Section 5 is similar to Section 3, but they are for the convection-dispersion equations. Finally, the concluding remarks are presented in Section 6.

2. The IMEX finite difference schemes for the convection-diffusion equations

Consider the linear convection-diffusion equation

$$(1) \qquad \begin{cases} u_t + u_x = du_{xx}, & (x,t) \in (a,b) \cup (0,T], \\ u(x,0) = u_0(x), & x \in [a,b], \end{cases}$$

with periodic boundary condition, where $d \geq 0$ is the diffusion coefficient. Assume that $[a,b]$ is uniformly partitioned into N cells with the spatial mesh size given by $\Delta x = \frac{b-a}{N}$. For the spatial discretization, we use the third order upwind biased finite difference scheme for the convection term, which is just the standard third

order WENO scheme with the linear weights, and the fourth order central difference method for the diffusion term to get the semidiscrete scheme,

$$(2) \qquad \frac{du}{dt}\bigg|_{x=x_i} = L(t,u)_i + N(t,u)_i,$$

in which $N(t,u)_i$ represents the spatial discretization of the convection term

$$(3) \qquad N(t,u)_i = -\frac{3u_i + 2u_{i+1} - 6u_{i-1} + u_{i-2}}{6\Delta x},$$

and $L(t,u)_i$ represents the spatial discretization of the diffusion term

$$(4) \qquad L(t,u)_i = d\,\frac{-(u_{i+2} + u_{i-2}) + 16(u_{i+1} + u_{i-1}) - 30u_i}{12\Delta x^2}.$$

The numerical solution u_i approximates the exact solution $u(x,t)$ at the grid point x_i. In the following subsections, we will consider two types of IMEX time-marching methods, i.e., Runge-Kutta and multistep methods given in [17]. We will give the stability analysis on these two high order IMEX methods coupled with the above finite difference spatial discretization by the Fourier method. Numerical experiments are also given to demonstrate the stability results given by our analysis.

2.1. The third order IMEX Runge-Kutta finite difference scheme. Let $\{t^n = n\Delta t \in [0,T]\}_{n=0}^M$ be the time at the n-th time step, in which Δt is the time step. Given u^n, the third order IMEX Runge-Kutta time-marching method [17] coupled with the above finite difference spatial discretization is given in the following form

$$(5) \qquad \begin{cases} u^{(1)} = u^n \\ u^{(s)} = u^n + \Delta t \displaystyle\sum_{j=2}^{s} a_{sj} L(t_j^n, u^{(j)}) + \Delta t \displaystyle\sum_{j=1}^{s-1} \hat{a}_{sj} N(t_j^n, u^{(j)}) \\ u^{n+1} = u^n + \Delta t \displaystyle\sum_{j=2}^{4} b_j L(t_j^n, u^{(j)}) + \Delta t \displaystyle\sum_{j=1}^{4} \hat{b}_j N(t_j^n, u^{(j)}) \end{cases}, \quad 2 \le s \le 4,$$

where $u^{(s)}$ approximates $u(t^n + c_s\Delta t)$, $c_s = \sum_{j=2}^{s} a_{sj} = \sum_{j=1}^{s-1} \hat{a}_{sj}$, and $t_j^n = t^n + c_j\Delta t$. The Butcher coefficients $a_{sj}, \hat{a}_{sj}, b_j,$ and $\hat{b}_j$ of (5) are specified in the following table.

$$(6)$$

a_{sj}	0	0	0	0	0	0	0	0	$\hat{a}_{sj}$
	0	γ	0	0	γ	0	0	0	
	0	$\dfrac{1-\gamma}{2}$	γ	0	$\dfrac{1+\gamma}{2} - \alpha_1$	α_1	0	0	
	0	β_1	β_2	γ	0	$1-\alpha_2$	α_2	0	
b_j	0	β_1	β_2	γ	0	$1-\alpha_2$	α_2	0	$\hat{b}_j$

The left half of the table lists a_{sj} and b_j, with the four rows from top to bottom corresponding to $s = 1,2,3,4$, and the columns from left to right corresponding to $j = 1,2,3,4$. Similarly, the right half lists $\hat{a}_{sj}$ and $\hat{b}_j$ in (6), $\gamma \approx 0.435866521508459$, $\beta_1 = -\frac{3}{2}\gamma^2 + 4\gamma - \frac{1}{4}$ and $\beta_2 = \frac{3}{2}\gamma^2 - 5\gamma + \frac{5}{4}$. The parameter α_1 is chosen as -0.35 in [16] and $\alpha_2 = \frac{\frac{1}{3} - 2\gamma^2 - 2\beta_2\alpha_1\gamma}{\gamma(1-\gamma)}$.

2.1.1. Stability analysis. We know that when the spatial discretization operator is LDG, the IMEX schemes [16, 17] are shown to be stable as long as the time step is upper-bounded by a constant, which depends on the ratio of the diffusion coefficient and the square of the convection coefficient. For the IMEX Runge-Kutta finite difference scheme (5), we expect to obtain similar stability, that is, the scheme could be stable under the condition $\Delta t \leq \tau_0$, where τ_0 is a positive constant depending solely on the diffusion coefficient d (notice that the convection coefficient is the constant 1). Next, we would like to explore whether the scheme would allow us to achieve such stability by the aid of the Fourier method.

The Fourier method, which is a powerful tool for stability analysis, consists of examining the following Fourier modes

$$(7) \qquad u_j^n = v^n e^{Ikx_j}, \quad I^2 = -1,$$

for appropriate wave number k. Substituting (7) into (5) yields

$$(8) \qquad v^{n+1} = Gv^n,$$

where the amplification factor G is a function of $k, \Delta x, \Delta t, d$. The specific formula of G for the scheme (5) is listed in Appendix A. The necessary and sufficient stability condition on G is given by the following theorem.

Theorem: *(von Neumann condition) Consider the difference approximation shown in (8), where G is a scalar, on a finite interval $0 \leq n\Delta t \leq T$. Assume that $\mathbb{Z}$ is the set of all integers. If there is a constant K such that for all $k \in \mathbb{Z}$*

$$|G| \leq 1 + K\Delta t,$$

then the approximation is stable.

Because the L^2 norm of the exact solution to the equation (1) does not increase in time, we would look for strong stability, namely the von Neumann stability requirement is $|G| \leq 1$. If $|G| \leq 1$ holds for $\Delta t \leq \tau_0$, then the scheme is stable under the condition $\Delta t \leq \tau_0$. If τ_0 is a sharp bound, then $|G|$ will be greater than 1 when $\Delta t = \tau_0 + \varepsilon$ (we take $\varepsilon = 0.01$ in our tests). As shown in Appendix A, the specific formula for G is very complex. Thus it is difficult to obtain τ_0 analytically. Considering the algebraic complexity, we will try to get it numerically. The specific procedure to obtain τ_0 is as follows.

To reduce the numerical error arisen from the calculation of Δx, in the code, we directly take Δx as $\frac{b-a}{2N}$. Besides, to reduce computational complexity, we only impose the condition $|G| \leq 1$ for each of the following discrete k values

$$(9) \qquad k = n_0, \quad n_0 = -N+1, -N+2, ..., N.$$

It is therefore a slightly looser condition than that required for all $k \in \mathbb{Z}$, but for large N the two conditions become essentially equivalent within $O(1/N^2)$ in general [11]. During the search for τ_0 we take $N = 10^5$. For each set of $\Delta t, N, k$, the value of $|G|$ is computed. By checking whether the inequality $|G| \leq 1$ is satisfied for all discrete k values in (9), we can get a range of the time step. The maximum value of this range is recorded as τ_0. The code to determine the stability condition for the scheme (5) implemented in the Matlab is given in Appendix B. When the period is 2π, the maximum time step τ_0 for the different diffusion coefficient d is listed in Table 2. Fig. 1 shows the approximately linear relationship between d and τ_0, which can be described as

$$\tau_0 \approx 4.859d.$$

TABLE 2. *The maximum time step τ_0.*

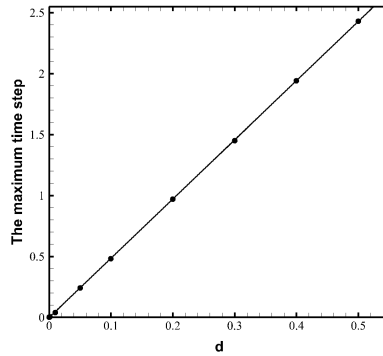| d	0	0.0001	0.001	0.01	0.05	0.1	0.2	0.3	0.4	0.5
τ_0	0	0.0005	0.004	0.04	0.24	0.48	0.97	1.45	1.94	2.43

FIGURE 1. *The fitting curve of the maximum time step τ_0 and the diffusion coefficient d.*

Notice that when d is very small or even zero, τ_0 would be too small to be the true bound for stability, because this scheme can also be stable under the standard CFL condition

$$(10) \qquad \Delta t \leq c\Delta x,$$

if the diffusion term is not considered. Next, we would like to further find the possible CFL-like stability condition (10) for the scheme (5).

Similarly, we obtain c in (10) numerically. When $d = 0$, we get the Courant number c as follows,

$$c = 1.3599.$$

We also observe the following two important facts.

1. When $\max\{c\Delta x, \tau_0\} = \tau_0$, $|G| \leq 1$ holds. When $\Delta t = \tau_0 + 0.01$, $|G|$ tends to be greater than 1.
2. For $d > 0$, we find that $c = 1.3599$ may not be the optimal Courant number; that is, $|G|$ may not be greater than 1 if we take $\Delta t = (c + 0.01)\Delta x$. But for any d, it seems sufficient to ensure that if $\Delta t = \max\{c\Delta x, \tau_0\} = c\Delta x$, then $|G| \leq 1$.

Therefore, we conclude that the third order IMEX Runge-Kutta finite difference scheme (5) is stable under the condition

$$(11) \qquad \Delta t \leq \max\{\tau_0, c\Delta x\},$$

where $\tau_0 \approx 4.859d, c = 1.3599$.

In order to further verify whether the scheme is subject to the above time step restriction, we consider the following equation

$$(12) \qquad \begin{cases} u_t + u_x = du_{xx}, & (x, t) \in (-\pi, \pi) \cup (0, T], \\ u(x, 0) = \sin x, & x \in [-\pi, \pi], \end{cases}$$

TABLE 3. *The error of the scheme* (5) *for solving the equation* (12) *with the different time step in the case of* $\max\{\tau_0, c\Delta x\} = \tau_0$, $\Delta x = \frac{2\pi}{N_{\tau_0}}$.

d	Δt	N_{τ_0}	T	L^1 error
	2.42			9.10E-14
d=0.5	2.43	640	50000	2.04E-14
	2.44			2.63E+16
	1.93			5.12E-14
d=0.4	1.94	640	50000	2.91E-14
	1.95			4.13E+07
	0.96			8.19E-15
d=0.2	0.97	640	10000	6.74E-15
	0.98			5.32E+08

TABLE 4. *The error of the scheme* (5) *for solving the equation* (12) *with the different time step in the case of* $\max\{\tau_0, c\Delta x\} = c\Delta x$, $\Delta x = \frac{2\pi}{N_c}$.

d	Δt	N_c	T	L^1 error
	$1.3499\Delta x$			0.537
d=0	$1.3599\Delta x$	40	10000	0.539
	$1.3699\Delta x$			3.88E+217
	$1.3499\Delta x$			0.1975
d=0.0001	$1.3599\Delta x$	40	10000	0.1982
	$1.3699\Delta x$			4.61E+157
	$1.3499\Delta x$			2.52E-16
d=0.001	$1.3599\Delta x$	40	100000	4.68E-16
	$1.3699\Delta x$			2.87E-16
	$1.3499\Delta x$			1.61E-16
d=0.01	$1.3599\Delta x$	40	100000	1.58E-16
	$1.3699\Delta x$			1.13E-16

with periodic boundary condition. The exact solution of (12) is $u(x,t) = e^{-dt}\sin(x - t)$. We use the scheme (5) to solve the above equation.

On the one hand, we take $N_{\tau_0} = 640$ in the tests so that $\max\{c\Delta x, \tau_0\} = \tau_0$, where $\Delta x = \frac{2\pi}{N_{\tau_0}}$. For any fixed diffusion coefficient d, we take Δt as $\tau_0 - 0.01$, τ_0 and $\tau_0 + 0.01$, respectively. Table 3 lists the L^1 error of the scheme (5) for solving (12) with the different time step. As expected, the error will blow up if we take $\Delta t = \tau_0 + 0.01$ but is small when $\Delta t \leq \tau_0$. Therefore, when $\max\{c\Delta x, \tau_0\} = \tau_0$, τ_0 is the precise bound of the time step restriction for stability. This clearly demonstrates the stability result (11) given by our analysis in such situation.

On the other hand, we take $N_c = 40$ in the tests such that $\max\{c\Delta x, \tau_0\} = c\Delta x$, where $\Delta x = \frac{2\pi}{N_c}$. For any given diffusion coefficient d, we take the time step Δt as $(c-0.01)\Delta x$, $c\Delta x$ and $(c+0.01)\Delta x$, respectively. We can clearly observe from Table 4 that when d is small enough, the error will blow up if we take $\Delta t = (c + 0.01)\Delta x$ but is tolerable under the condition $\Delta t \leq c\Delta x$, and when d is relatively larger, the error will not blow up when $\Delta t = (c + 0.01)\Delta x$, which verifies our observation in the stability analysis.

Thus, combining the results in Tables 3-4, we conclude that the third order IMEX Runge-Kutta finite difference scheme (5) is stable under the time step restriction (11).

2.2. The third order multistep IMEX finite difference scheme. Considering the semidiscrete scheme (2), we use the third order multistep IMEX time-marching method given in [17] to discretize it to obtain a finite difference scheme as follows

$$
\begin{aligned}
(13) \quad u_i^{n+1} =& u_i^n + \Delta t\Big(\frac{23}{12}N(t^n, u^n)_i - \frac{4}{3}N(t^{n-1}, u^{n-1})_i + \frac{5}{12}N(t^{n-2}, u^{n-2})_i\Big) \\
& + \Delta t\Big(\frac{2}{3}L(t^{n+1}, u^{n+1})_i + \frac{5}{12}L(t^{n-1}, u^{n-1})_i - \frac{1}{12}L(t^{n-3}, u^{n-3})_i\Big),
\end{aligned}
$$

where $N(t, u)_i$ and $L(t, u)_i$ are defined as (3) and (4) respectively. Next, we will perform the stability analysis on this scheme.

2.2.1. Stability analysis. When the spatial discretization operator is LDG, we know that the multistep IMEX schemes [17] are shown to be stable provided that the time step is upper-bounded by a positive constant, which depends on the ratio of the diffusion coefficient and the square of the convection coefficient. For the multistep IMEX finite difference scheme (13), we expect to obtain similar stability, that is, the scheme could also be stable under the condition $\Delta t \leq \tau_0$, where τ_0 is a positive constant proportional to the diffusion coefficient d. Next, we would like to explore whether the scheme can achieve such stability by the aid of the Fourier method.

Substituting the Fourier modes (7) into the scheme, we obtain

$$
(14) \qquad v^{n+1} = a_1 v^n + a_2 v^{n-1} + a_3 v^{n-2} + a_4 v^{n-3}.
$$

The specific formulas for $a_i, i = 1, .., 4$ are listed in Appendix A.

To solve (14), we make the ansatz

$$
(15) \qquad v^n = z^n,
$$

where z is a complex number. Substituting (15) into (14) gives us

$$
z^{n+1} - a_1 z^n - a_2 z^{n-1} - a_3 z^{n-2} - a_4 z^{n-3} = 0.
$$

Therefore, (15) is a solution of (14) if, and only if, z satisfies the so called characteristic equation

$$
(16) \qquad z^4 - a_1 z^3 - a_2 z^2 - a_3 z - a_4 = 0.
$$

The necessary and sufficient stability condition on the characteristic root z is defined as follows.

Theorem: *Consider the difference approximation shown in (14) on a finite interval $0 \leq n\Delta t \leq T$. Assume that $\mathbb{Z}$ is the set of all integers. If there is a constant K such that for all $k \in \mathbb{Z}$*

$$
\begin{cases}
|z| < 1, & \text{if } z \text{ is a multiple root,} \\
|z| \leq 1 + K\Delta t, & \text{else,}
\end{cases}
$$

then the approximation is stable.

Applying to the case of interest here, we would like to derive the values of τ_0 for strong stability, namely

$$
(17) \qquad
\begin{cases}
|z| \leq 1, & \text{when } z \text{ is a simple root of (16),} \\
|z| < 1, & \text{when } z \text{ is a multiple root of (16).}
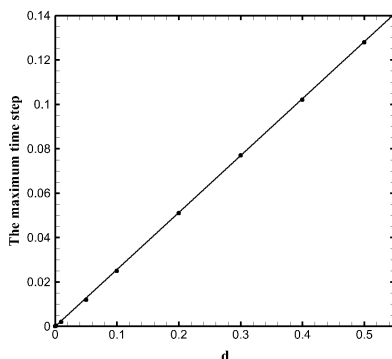\end{cases}
$$

FIGURE 2. *The fitting curve of the maximum time step τ_0 and the diffusion coefficient d.*

since the L^2 norm of the exact solution to the equation (1) does not increase in time. Considering the algebraic complexity, we still get τ_0 numerically. When the period is 2π, the maximum time step τ_0 is obtained in the similar way as that for the third order IMEX Runge-Kutta finite difference scheme (5). We refer to Section 2.1.1 for more details. Here we just summarize the result in Table 5.

TABLE 5. *The maximum time step τ_0.*

d	0	0.001	0.01	0.05	0.1	0.2	0.3	0.4	0.5
τ_0	0	0.0002	0.002	0.012	0.025	0.051	0.077	0.103	0.128

Similarly Fig. 2 shows the approximately linear relationship between d and τ_0, which can be expressed as

$$(18) \qquad\qquad\qquad \tau_0 \approx 0.2566d.$$

We observe that the IMEX Runge-Kutta finite difference scheme (5) admits larger time step than the multistep IMEX finite difference scheme (13). Similar to the scheme (5), when d is very small in comparison with the spatial mesh size, τ_0 determined by (18) is too small to be true for stability. Thus, we will further find the similar CFL-like stability condition for the scheme (13).

In order to get stability, c should satisfy (17). We get the value of c numerically. When $d = 0$, we obtain $c = 0.39$, that is, the scheme is stable when the time step satisfies

$$\Delta t \leq 0.39\Delta x.$$

Besides, we also observe the following two important facts.

1. When $\max\{c\Delta x, \tau_0\} = \tau_0$, (17) holds if $\Delta t \leq \tau_0$. If we take $\Delta t = \tau_0 + 0.01$, the roots of the characteristic equation will lie outside the complex unit disk.
2. When $d > 0$, $c = 0.39$ may not be the optimal Courant number, that is, the roots of the characteristic equation may not lie outside the complex unit disk if we take $\Delta t = (c + 0.01)\Delta x$. However, it seems sufficient to ensure that (17) holds if $\Delta t = \max\{c\Delta x, \tau_0\} = c\Delta x$ for any d.

TABLE 6. *The error of the scheme* (13) *for solving* (12) *with the different time step in the case of* $\max\{\tau_0, c\Delta x\} = \tau_0$, $\Delta x = \frac{2\pi}{N_{\tau_0}}$.

d	Δt	N_{τ_0}	T	L^1 error
d=0.5	0.127	640	30000	7.20E-15
	0.128			8.42E-16
	0.129			1.22E+29
d=0.4	0.102	640	30000	6.68E-14
	0.103			6.11E-14
	0.104			1.16E+161
d=0.2	0.05	640	30000	6.09E-15
	0.051			6.16E-14
	0.052			9.30E+303

Therefore, we conclude that the third order multistep IMEX finite difference scheme (13) is stable under the condition

$$(19) \qquad\qquad \Delta t \leq \max\{\tau_0, c\Delta x\},$$

where $\tau_0 \approx 0.2566d$, $c = 0.39$.

In order to further verify whether the scheme is subject to the above time step restriction (19), we still verify it on the equation (12). Since the third order multistep IMEX finite difference scheme is not self-starting, we adopt the third order IMEX Runge-Kutta finite difference scheme (5) to compute the solutions at the first three time levels.

We first take $N_{\tau_0} = 640$ in the test such that $\max\{c\Delta x, \tau_0\} = \tau_0$, where $\Delta x = \frac{2\pi}{N_{\tau_0}}$. For any fixed diffusion coefficient d, we take Δt as $\tau_0 - 0.001$, τ_0 and $\tau_0 + 0.001$ respectively. Table 6 lists the L^1 error of the scheme (13) solving (12) with the different time step. As expected, the error will blow up if we take $\Delta t = \tau_0 + 0.001$ but is small when $\Delta t \leq \tau_0$. Therefore, when $\max\{c\Delta x, \tau_0\} = \tau_0$, τ_0 is the precise bound of time step restriction for stability. This verifies the stability result produced by our analysis.

Then we take $N_c = 40$ in the test so that $\max\{c\Delta x, \tau_0\} = c\Delta x$, where $\Delta x = \frac{2\pi}{N_c}$. For any given diffusion coefficient d, we take the time step Δt as $(c-0.01)\Delta x$, $c\Delta x$ and $(c+0.01)\Delta x$ respectively. When d is relatively large, the L^1 norm of the error does not blow up even in the case $\Delta t = (c+0.01)\Delta x$, as shown in Table 7. When d is sufficiently small, we can clearly observe that the error will blow up if we take $\Delta t = (c+0.01)\Delta x$ but is tolerable under the condition $\Delta t \leq c\Delta x$. This clearly demonstrates the stability result predicted by our analysis.

Therefore, we conclude that the third order multistep IMEX finite difference scheme (13) is stable under the condition (19).

3. Numerical experiments

The purpose of this section is to numerically validate the error accuracy of the third order IMEX Runge-Kutta finite difference scheme (5) and the third order multistep IMEX finite difference scheme (13) under the above discussed stability conditions. In the implementation of the multistep IMEX finite difference scheme, we use the IMEX Runge-Kutta finite difference scheme to compute the solutions at the first three time levels. In the experiments, we will take the final computing time $T = 10$ and the diffusion coefficient $d = 0.5$, unless otherwise stated.

TABLE 7. *The error of the scheme* (13) *for solving* (12) *with the different time step in the case of* $\max\{\tau_0, c\Delta x\} = c\Delta x$, $\Delta x = \frac{2\pi}{N_c}$.

d	Δt	N_c	T	L^1 error
	$0.38\Delta x$			0.2259
d=0	$0.39\Delta x$	40	1000	0.2288
	$0.40\Delta x$			9.34E+39
	$0.38\Delta x$			0.0831
d=0.001	$0.39\Delta x$	40	1000	0.0842
	$0.40\Delta x$			1.58E+06
	$0.38\Delta x$			2.27E-16
d=0.01	$0.39\Delta x$	40	100000	1.50E-17
	$0.40\Delta x$			6.95E-16
	$0.38\Delta x$			6.41E-16
d=0.05	$0.39\Delta x$	40	100000	1.07E-15
	$0.40\Delta x$			3.44E-16

TABLE 8. *Error and order for the schemes* (5) *and* (13) *solving the equation* (12).

N	IMEX Runge-Kutta scheme				multistep IMEX scheme			
	L^1 error	order	L^∞ error	order	L^1 error	order	L^∞ error	order
40	1.46E-05		2.31E-05		1.49E-05		2.34E-05	
80	1.79E-06	3.03	2.83E-06	3.03	1.83E-06	3.03	2.87E-06	3.03
160	2.22E-07	3.01	3.49E-07	3.02	2.30E-07	2.99	3.61E-07	2.99
320	2.76E-08	3.01	4.34E-08	3.01	2.78E-08	3.05	4.36E-08	3.05
640	3.44E-09	3.00	5.41E-09	3.00	3.41E-09	3.02	5.36E-09	3.02
1280	4.30E-10	3.00	6.76E-10	3.00	4.69E-10	2.86	7.36E-10	2.86

First, consider the linear equation (12). For the third order IMEX Runge-Kutta finite difference scheme (5) and the third order multistep IMEX finite difference scheme (13), we take the time step $\Delta t = 0.6\Delta x$ and $\Delta t = 0.1\Delta x$ respectively. The L^1 and L^∞ error and order of accuracy are contained in Table 8. We can clearly observe the designed order of accuracy from this table.

In order to test the order of accuracy with respect to time, we take $N = 2560$ and the proper time step so that the temporal error is always dominant. The L^1 and L^∞ error and order of accuracy for the schemes (5) and (13) solving the equation (12) can be observed from Table 9. The optimal order of accuracy can be observed in this table.

Although we only perform the stability analysis on the linear convection-diffusion equations, numerical experiments show that the obtained stability conditions are also applicable to the equations with the nonlinear convection term. Next, we will perform the test on the nonlinear Burgers' equation,

$$(20) \quad \begin{cases} u_t + (\frac{u^2}{2})_x = 0, & (x,t) \in (-\pi, \pi) \cup (0, T], \\ u(x,0) = \frac{1}{2} + \sin x, & x \in [-\pi, \pi], \end{cases}$$

with the periodic boundary condition. Even though the initial condition is quite smooth, the solution of the equation will become discontinuous in finite time. The third order upwind biased finite difference scheme, which is the standard third order

TABLE 9. *The error and order for the schemes* (5) *and* (13) *solving the equation* (12), $N = 2560$.

Δt	IMEX Runge-Kutta scheme			
	L^1 error	order	L^∞ error	order
0.6	3.27E-04		5.14E-04	
0.3	4.88E-05	2.75	7.66E-05	2.75
0.15	6.64E-06	2.88	1.04E-05	2.88
0.075	8.68E-07	2.93	1.36E-06	2.93
0.0375	1.11E-07	2.97	1.74E-07	2.97
0.01875	1.40E-08	2.98	2.20E-08	2.98
Δt	multistep IMEX scheme			
	L^1 error	order	L^∞ error	order
0.1	2.55E-05		4.01E-05	
0.05	3.17E-06	3.01	4.98E-06	3.01
0.025	3.95E-07	3.01	6.20E-07	3.01
0.0125	4.93E-08	3.00	7.73E-08	3.00
0.00625	6.18E-09	3.00	9.70E-09	2.99
0.003125	8.01E-10	2.95	1.26E-09	2.95
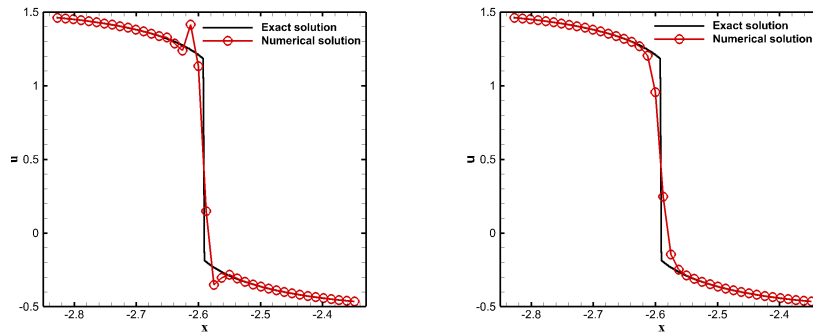
FIGURE 3. *The third order upwind biased scheme (left) and the third order multi-resolution WENO scheme (right) for the Burgers' equation. Solid line: exact solution; Circle symbol: the numerical solution at $T = 1.1$. $N = 500$.*

WENO scheme [12, 14] with linear weights (when the smoothness indicators and nonlinear weights are turned off), produces oscillations near the discontinuity, see the left figure of Fig 3. The multi-resolution WENO scheme [20] is a good choice to eliminate or reduce the oscillations near the discontinuity, see the right figure of Fig 3.

For the Burgers' equation, we consider both the third order upwind biased scheme and the third order multi-resolution WENO scheme for the spatial discretization. In order to ensure correct upwind biasing and stability, a simple Lax-Friedrichs flux splitting [15] is used. We take $\Delta t = 0.6\Delta x$ for the scheme with the IMEX Runge-Kutta time discretization and take $\Delta t = 0.1\Delta x$ for the scheme with the multistep IMEX time discretization. Tables 10 and 11 are the L^1 and L^∞ error

TABLE 10. *The error and order of the third order upwind biased scheme (left) and multi-resolution WENO scheme (right) coupled with the third order IMEX Runge-Kutta time discretization solving the equation* (20). *The time step is* $\Delta t = 0.6\Delta x$.

N	the upwind biased scheme				the multi-resolution WENO scheme			
	L^1 error	order	L^∞ error	order	L^1 error	order	L^∞ error	order
80	7.32E-05		5.67E-04		7.91E-04		7.00E-03	
160	8.15E-06	3.17	6.66E-05	3.09	1.82E-04	2.12	2.60E-03	1.43
320	9.52E-07	3.10	7.99E-06	3.06	3.56E-05	2.36	8.95E-04	1.55
640	1.15E-07	3.05	9.73E-07	3.04	5.84E-06	2.61	2.69E-04	1.73
1280	1.41E-08	3.03	1.20E-07	3.02	6.51E-07	3.16	5.97E-05	2.17
2560	1.75E-09	3.01	1.49E-08	3.01	5.53E-08	3.56	8.71E-06	2.78

TABLE 11. *The error and order of the third order upwind biased scheme (left) and multi-resolution WENO scheme (right) coupled with the third order multistep IMEX time discretization solving the equation* (20). *The time step is* $\Delta t = 0.1\Delta x$.

N	the upwind biased scheme				the multi-resolution WENO scheme			
	L^1 error	order	L^∞ error	order	L^1 error	order	L^∞ error	order
80	6.59E-04		4.40E-03		7.16E-04		6.20E-03	
160	6.98E-05	3.24	5.36E-04	3.03	1.61E-04	2.15	2.30E-03	1.43
320	7.86E-06	3.15	6.27E-05	3.10	3.28E-05	2.30	8.15E-04	1.51
640	9.24E-07	3.09	7.43E-06	3.08	5.32E-06	2.62	2.42E-04	1.75
1280	1.12E-07	3.05	9.03E-07	3.04	6.10E-07	3.12	5.47E-05	2.14
2560	1.38E-08	3.02	1.11E-07	3.02	5.54E-08	3.46	8.27E-06	2.73

and order of accuracy for the above mentioned schemes. We compute the solution up to $T = 0.5$ in the test, when the solution is still smooth. The optimal order of accuracy can be observed from both tables.

Finally, we consider the viscous Burgers' equation [16] with a source term

$$
(21) \qquad \begin{cases} u_t + (\dfrac{u^2}{2})_x = du_{xx} + g(x,t), & (x,t) \in (-\pi, \pi) \cup (0, T], \\ u(x,0) = \sin x, & x \in [-\pi, \pi]. \end{cases}
$$

The source term is $g(x,t) = \frac{1}{2}e^{-2dt}\sin(2x)$, and the exact solution is $u(x,t) = e^{-dt}\sin(x)$. In order to ensure correct upwind biasing and stability, a simple Lax-Friedrichs flux splitting is used for the convection term. For the third order IMEX Runge-Kutta finite difference scheme (5) and the third order multistep IMEX finite difference scheme (13), we take the time step $\Delta t = 0.6\Delta x$ and $\Delta t = 0.1\Delta x$, respectively. Then we can again clearly observe the designed order of accuracy for the schemes solving the equation (21) in Table 12.

TABLE 12. *The error and order for the schemes* (5) *and* (13) *solving the equation* (21).

N	IMEX Runge-Kutta				multistep IMEX			
	L^1 error	order	L^∞ error	order	L^1 error	order	L^∞ error	order
100	1.62E-07		2.57E-07		1.59E-07		2.53E-07	
200	2.05E-08	2.98	3.24E-08	2.99	2.03E-08	2.97	3.20E-08	2.98
300	6.11E-09	2.99	9.63E-09	2.99	6.11E-09	2.96	9.63E-09	2.96
400	2.58E-09	2.99	4.07E-09	3.00	2.61E-09	2.96	4.11E-09	2.96
500	1.32E-09	2.99	2.09E-09	3.00	1.33E-09	3.02	2.09E-09	3.02
600	7.67E-10	3.00	1.21E-09	3.00	7.94E-10	2.83	1.25E-09	2.83

4. The IMEX finite difference schemes for the convection-dispersion equations

In this section, we will extend our work in Section 2 to the linear convection-dispersion equation

$$(22) \qquad \begin{cases} u_t + u_x + d u_{xxx} = 0, & (x,t) \in (a,b) \cup (0,T], \\ u(x,0) = u_0(x), & x \in [a,b], \end{cases}$$

with periodic boundary condition, where the dispersion coefficient $d \geq 0$ is a constant. Since this is a wave equation and the third order derivative term $d u_{xxx}$ does not provide any diffusion to help control the convection term u_x, we do not expect a better stability condition for $d > 0$ than for $d = 0$. This is different from the situation of convection-diffusion equations discussed in previous sections. In this section, we will focus our attention on the stability analysis for the third order IMEX Runge-Kutta method [16], the third order additive Runge-Kutta method [10] and the second order multistep IMEX method [17] coupled with certain high order finite difference spatial discretization respectively. Numerical experiments are also given to demonstrate the stability results given by the analysis.

4.1. The spatial discretization. In this subsection, we present the spatial discretization of (22). We adopt the third order upwind biased finite difference scheme, which is a prototype of the third order WENO scheme to discretize the convection term, and the third order one-point upwind biased scheme to discretize the dispersion term. Then we can get the following semidiscrete scheme

$$(23) \qquad \left. \frac{du}{dt} \right|_{x=x_i} = \mathcal{L}(t,u)_i + N(t,u)_i,$$

where $\mathcal{L}(t,u)_i$ arises from the spatial discretization of the dispersion term

$$(24) \qquad \mathcal{L}(t,u)_i = -d \, \frac{-u_{i+3} + 7u_{i+2} - 14u_{i+1} + 10u_i - u_{i-1} - u_{i-2}}{4\Delta x^3},$$

and $N(t,u)_i$ is derived from the spatial discretization of the convection term. The specific formula for $N(t,u)_i$ is given by (3).

4.2. The temporal discretization. In this subsection, we consider the fully discrete schemes for the ODE system (23). Both Runge-Kutta and multistep IMEX time-marching methods are considered. For a detailed introduction to IMEX time-marching methods, please refer to [13, 16, 17].

4.2.1. The third order Runge-Kutta type finite difference scheme. We use the third order IMEX Runge-Kutta method [16] and the third order additive Runge-Kutta method [10] to fully discretize the semidiscrete scheme (23) and obtain

$$
\begin{cases}
u^{(1)} = u^n \\
u^{(i)} = u^n + \Delta t \sum_{j=1}^{i} a_{ij}\mathcal{L}(t_j^n, u^{(j)}) + \Delta t \sum_{j=1}^{i-1} \hat{a}_{ij} N(t_j^n, u^{(j)}) \\
u^{n+1} = u^n + \Delta t \sum_{j=1}^{4} b_j \mathcal{L}(t_j^n, u^{(j)}) + \Delta t \sum_{j=1}^{4} \hat{b}_j N(t_j^n, u^{(j)})
\end{cases}
, 2 \le i \le 4,
$$

where $t_i^n = t^n + c_i \Delta t$, $u^{(i)}$ approximates $u(t_i^n)$. The third order IMEX Runge-Kutta method has been described in detail in the previous subsection for solving the convection-diffusion equations. For details on the Butcher coefficients of this method, please refer to (6). The coefficients of the additive Runge-Kutta method are given in the following tabular data.

(25)

a_{ij}	0	0	0	0
	γ	γ	0	0
	$\frac{2746238789719}{10658868560708}$	$\frac{-640167445237}{6845629431997}$	γ	0
	$\frac{1471266399579}{7840856788654}$	$\frac{-4482444167858}{7529755066697}$	$\frac{11266239266428}{11593286722821}$	γ
b_i	$\frac{1471266399579}{7840856788654}$	$\frac{-4482444167858}{7529755066697}$	$\frac{11266239266428}{11593286722821}$	γ
c_i	0	2γ	$\frac{3}{5}$	1

$\hat{a}_{ij}$	0	0	0	0
	2γ	0	0	0
	$\frac{5535828885825}{10492691773637}$	$\frac{788022342437}{10882634858940}$	0	0
	$\frac{6485989280629}{16251701735622}$	$\frac{-4246266847089}{9704473918619}$	$\frac{10755448449292}{10357097424841}$	0
$\hat{b}_i$	$\frac{1471266399579}{7840856788654}$	$\frac{-4482444167858}{7529755066697}$	$\frac{11266239266428}{11593286722821}$	γ

The first table in (25) lists a_{ij}, b_j and c_i, with the four rows from top to bottom corresponding to $i = 1, 2, 3, 4$, and the columns from left to right corresponding to $j = 1, 2, 3, 4$ respectively. Similarly, the second table lists $\hat{a}_{ij}$ and $\hat{b}_j$. In (25), the value of γ is set as $\frac{1767732205903}{4055673282236}$.

The additive Runge-Kutta method is a combination of the traditional explicit Runge-Kutta method and an L-stable, stiffly-accurate, singly diagonally implicit Runge-Kutta method. Compared with the IMEX Runge-Kutta finite difference scheme of the same order which has the advantage of simplicity, the additive Runge-Kutta finite difference scheme exhibits excellent stability in the existence of stiffness [13].

4.2.2. The second order multistep IMEX finite difference scheme. Because no multistep method of order greater than 2 can be A-stable [7], we will consider the second order multistep IMEX time-marching method [17] with an A-stable trapezoidal rule for the implicit part in this paper. The finite difference scheme is in the form

(26)
$$
\begin{aligned}
u_i^{n+1} - u_i^n = &\Delta t \left(\frac{3}{2} N(t^n, u^n)_i - \frac{1}{2} N(t^{n-1}, u^{n-1})_i \right) + \\
&\Delta t \left(\frac{3}{4} \mathcal{L}(t^{n+1}, u^{n+1})_i + \frac{1}{4} \mathcal{L}(t^{n-1}, u^{n-1})_i \right),
\end{aligned}
$$

TABLE 13. *The Courant number c.*

scheme	c
(6)	1.3599
(25)	2.03
(26)	0.58

where $N(t, u)_i$ stems from the spatial discretization of the convection term and $\mathcal{L}(t, u)_i$ arises from the spatial discretization of the dispersion term. The formulas for $N(t, u)_i$ and $\mathcal{L}(t, u)_i$ are specified in (3) and (24), respectively. In the following subsection, we would like to analyze the stability of the above schemes.

4.3. Stability analysis. In [5], some IMEX Runge-Kutta methods coupled with the finite volume spatial discretization are shown to be stable for the KdV equation under the standard CFL condition $\Delta t \leq c\Delta x$. For the IMEX schemes (6), (25), (26) coupled with finite difference spatial discretizations solving the linear convection-dispersion equation, in which we treat the dispersion term implicitly and the convection term explicitly, we can reasonably expect to obtain similar stability. Because of the algebraic complexity, we will proceed in the similar way as that in Section 2.1.1 to get the values of c. When the period is 2π and $d = 0$, Table 13 lists the maximum Courant number c which can guarantee the stability. We also find that when $d > 0$, c may not be the optimal Courant number in the sense that, if we take $\Delta t = (c + 0.01)\Delta x$, the norm of the amplification factor may not be greater than 1 (or the roots of the characteristic equation may not lie outside the complex unit disk), but we can ensure that $|G| \leq 1$ (or (17)) holds if $\Delta t \leq c\Delta x$ for any d.

In order to further verify whether the above listed c can ensure the numerical stability of the schemes, we consider the following equation

$$(27) \qquad \begin{cases} u_t + u_x + du_{xxx} = 0, & (x, t) \in (-\pi, \pi) \cup (0, T], \\ u(x, 0) = \sin(x), & x \in [-\pi, \pi], \end{cases}$$

with periodic boundary condition. The exact solution is $u(x, t) = \sin\big(x - (1 - d)t\big)$. Since the second order multistep IMEX finite difference scheme (26) is not self-starting, we adopt the third order IMEX Runge-Kutta finite difference scheme (6) to compute the solution at the first time level. In the tests, we take the time step Δt as $(c - 0.01)\Delta x$, $c\Delta x$ and $(c + 0.01)\Delta x$, respectively. Tables 14, 15 and 16 show that when $d = 0$, the error will blow up if we take $\Delta t = (c + 0.01)\Delta x$, but is tolerable under the condition $\Delta t \leq c\Delta x$. When $d \neq 0$, the L^1 and L^∞ error is bounded as shown in these three tables.

In general, these three schemes are stable under the standard CFL condition. Besides, it is worth noting that the Runge-Kutta type IMEX finite difference schemes (6), (25) admit larger time step than the multistep IMEX finite difference scheme (26), and the additive Runge-Kutta finite difference scheme (25) admits larger time step than the IMEX Runge-Kutta finite difference scheme (6).

5. Numerical experiments

In this section, we provide a few numerical examples, including the linear and nonlinear convection-dispersion problems, to illustrate stability condition and the error accuracy for the third order IMEX Runge-Kutta finite difference scheme (6), the third order additive Runge-Kutta finite difference scheme (25) and the second

TABLE 14. *The error of the scheme* (6) *for solving the equation* (27) *with the different time step.*

d	Δt	N_c	T	L^1 error	L^∞ error
d=0	$1.3499\Delta x$	40	10000	0.5370	0.8446
	$1.3599\Delta x$			0.5390	0.8471
	$1.3699\Delta x$			3.88E+217	6.20E+217
d=0.001	$1.3499\Delta x$	40	100000	0.6325	0.9996
	$1.3599\Delta x$			0.6325	0.9996
	$1.3699\Delta x$			0.6325	0.9996
d=0.01	$1.3499\Delta x$	40	100000	0.6420	1
	$1.3599\Delta x$			0.6420	1
	$1.3699\Delta x$			0.6420	1
d=0.05	$1.3499\Delta x$	40	100000	0.6451	0.9996
	$1.3599\Delta x$			0.6451	0.9996
	$1.3699\Delta x$			0.6451	0.9996

TABLE 15. *The error of the scheme* (25) *for solving the equation* (27) *with the different time step.*

d	Δt	N_c	T	L^1 error	L^∞ error
d=0	$2.02\Delta x$	40	10000	0.6281	0.9993
	$2.03\Delta x$			0.6281	0.9993
	$2.04\Delta x$			2.16E+51	3.21E+51
d=0.001	$2.02\Delta x$	40	100000	0.6325	0.9996
	$2.03\Delta x$			0.6325	0.9996
	$2.04\Delta x$			0.6325	0.9996
d=0.01	$2.02\Delta x$	40	100000	0.642	1
	$2.03\Delta x$			0.642	1
	$2.04\Delta x$			0.642	1
d=0.05	$2.02\Delta x$	40	100000	0.6451	0.9996
	$2.03\Delta x$			0.6451	0.9996
	$2.04\Delta x$			0.6451	0.9996

TABLE 16. *The error of the scheme* (26) *for solving* (27) *with the different time step.*

d	Δt	N_c	T	L^1 error	L^∞ error
d=0	$0.57\Delta x$	40	1000	1.1745	1.8248
	$0.58\Delta x$			1.1651	1.8086
	$0.59\Delta x$			3.45E+82	5.35E+82
d=0.001	$0.57\Delta x$	40	100000	0.6325	0.9996
	$0.58\Delta x$			0.6325	0.9996
	$0.59\Delta x$			0.6325	0.9996
d=0.01	$0.57\Delta x$	40	100000	0.642	1
	$0.58\Delta x$			0.642	1
	$0.59\Delta x$			0.642	1
d=0.05	$0.57\Delta x$	40	100000	0.6451	0.9996
	$0.58\Delta x$			0.6451	0.9996
	$0.59\Delta x$			0.6451	0.9996

TABLE 17. *The error and order for the schemes* (6), (25) *and* (26) *solving the equation* (27). $\Delta t = 0.5\Delta x$.

N	Norm	IMEX Runge-Kutta		Additive Runge-Kutta		multistep IMEX	
		error	order	error	order	error	order
40	L^1	3.90E-03		3.90E-03		9.50E-03	
	L^∞	6.10E-03		6.10E-03		1.50E-02	
60	L^1	1.10E-03	3.06	1.10E-03	3.06	4.00E-03	2.16
	L^∞	1.80E-03	3.05	1.80E-03	3.05	6.20E-03	2.15
80	L^1	4.71E-04	3.05	4.74E-04	3.05	2.20E-03	2.09
	L^∞	7.35E-04	3.04	7.40E-04	3.04	3.40E-03	2.09
100	L^1	2.39E-04	3.04	2.41E-04	3.04	1.40E-03	2.06
	L^∞	3.74E-04	3.03	3.76E-04	3.03	2.20E-03	2.06
120	L^1	1.38E-04	3.03	1.38E-04	3.03	9.43E-04	2.05
	L^∞	2.15E-04	3.03	2.17E-04	3.03	1.50E-03	2.05

order multistep IMEX finite difference scheme (26) respectively. In order to implement the scheme (26), we use the self-starting scheme (6) to compute the solution at the first time level.

Consider the linear convection-dispersion equation (27). We take $d = 0.5$, and the final computing time is $T = 10$. Table 17 lists the L^1 and L^∞ error and order of accuracy for these three schemes solving (27). We take $\Delta t = 0.5\Delta x$ in all the tests. Optimal order of accuracy can be observed in this table.

Although we only perform the stability analysis on the linear convection-dispersion equations, numerical experiments show that the stability conditions we obtained are also applicable to nonlinear equations. In the following, we would like to test the error and order of accuracy for the convection-dispersion equations with the nonlinear convection term. In order to ensure correct upwind biasing and stability, a simple Lax-Friedrichs flux [15] is used for the convection term.

First, we compute the classical soliton solution of the generalized KdV problem [19]

$$(28) \qquad \begin{cases} u_t + u_x + u^3 u_x + \epsilon u_{xxx} = 0, & (x,t) \in (-2,3) \cup (0,T], \\ u(x,0) = A \operatorname{sech}^{\frac{2}{3}}(K(x - x_0)), & x \in [-2,3], \end{cases}$$

where $\epsilon = 2.058 \times 10^{-5}$, $A = 0.2275$, $x_0 = 0.5$, $K = 3\left(\frac{A^3}{40\epsilon}\right)^{\frac{1}{2}}$. The exact solution is $u(x,t) = A \operatorname{sech}^{\frac{2}{3}}(K(x - x_0) - \omega t)$, $\omega = K(1 + \frac{A^3}{10})$. We take $\Delta t = 0.3\Delta x$ in all the tests. We choose a large domain and use the exact solution to serve as the boundary condition. Then we can clearly observe the designed order of accuracy from Table 18.

Next, we compute the classical soliton solution of the KdV problem [19]

$$(29) \qquad \begin{cases} u_t - 3(u^2)_x + u_{xxx} = 0, & (x,t) \in (-10,12) \cup (0,T] \\ u(x,0) = -2 \operatorname{sech}^2(x), & x \in [-10,12] \end{cases}$$

The exact solution is $u(x,t) = -2 \operatorname{sech}^2(x - 4t)$. We take $\Delta t = 0.1\Delta x$ in all the tests. Table 19 gives the L^1 and L^∞ error and order of accuracy at $T = 0.5$ using the exact solution to serve as the boundary condition. The optimal order of accuracy can be observed from this table.

TABLE 18. *The error and order for the schemes* (6), (25) *and* (26)
solving the equation (28). $\Delta t = 0.3\Delta x$.

N	Norm	IMEX Runge-Kutta		Additive Runge-Kutta		multistep IMEX	
		error	order	error	order	error	order
80	L^1	1.20E-03		1.20E-03		1.10E-03	
	L^∞	1.97E-02		1.98E-02		2.11E-02	
160	L^1	2.49E-04	2.23	2.52E-04	2.23	2.63E-04	2.07
	L^∞	6.50E-03	1.60	6.50E-03	1.60	7.00E-03	1.59
320	L^1	3.76E-05	2.73	3.80E-05	2.73	5.88E-05	2.16
	L^∞	1.30E-03	2.31	1.30E-03	2.30	1.70E-03	2.02
640	L^1	5.03E-06	2.90	5.09E-06	2.90	1.36E-05	2.12
	L^∞	1.91E-04	2.77	1.94E-04	2.77	3.88E-04	2.15
1280	L^1	6.35E-07	2.98	6.43E-07	2.98	3.34E-06	2.02
	L^∞	2.45E-05	2.97	2.47E-05	2.97	9.49E-05	2.03

TABLE 19. *The error and order for the schemes* (6), (25) *and* (26)
solving the equation (29). $\Delta t = 0.1\Delta x$.

N	Norm	IMEX Runge-Kutta		Additive Runge-Kutta		multistep IMEX	
		error	order	error	order	error	order
80	L^1	1.60E-02		1.61E-02		1.75E-02	
	L^∞	1.18E-01		1.20E-01		1.45E-01	
160	L^1	2.50E-03	2.68	2.50E-03	2.68	3.90E-03	2.18
	L^∞	1.79E-02	2.72	1.83E-02	2.71	3.05E-02	2.25
320	L^1	3.23E-04	2.95	3.28E-04	2.94	9.21E-04	2.07
	L^∞	2.30E-03	2.95	2.40E-03	2.94	6.90E-03	2.15
640	L^1	4.08E-05	2.99	4.15E-05	2.98	2.31E-04	1.99
	L^∞	2.88E-04	3.01	2.96E-04	3.01	1.70E-03	1.98
1280	L^1	5.11E-06	3.00	5.20E-06	3.00	5.84E-05	1.98
	L^∞	3.56E-05	3.01	3.66E-05	3.01	4.30E-04	2.02

Finally, we consider the soliton solution of the mKdV problem

$$(30) \qquad \begin{cases} u_t + 6u^2 u_x + u_{xxx} = 0, & (x,t) \in (-40, 40) \cup (0, T], \\ u(x,0) = \sqrt{c}\,\text{sech}(\sqrt{c}x), & x \in [-40, 40], \end{cases}$$

The exact solution is $u(x,t) = \sqrt{c}\,\text{sech}\left(\sqrt{c}(x - ct)\right)$. Here, we take $c = \frac{1}{2}$. We take $\Delta t = 0.1\Delta x$ in all the tests. Table 20 gives the L^1 and L^∞ error and order of accuracy at $T = 0.5$ using the exact solution to serve as the boundary condition. We can clearly observe the designed order of accuracy from this table.

6. Concluding remarks

We have considered some carefully chosen IMEX time marching methods coupled with high order finite difference spatial discretization for solving the linear convection-diffusion and the convection-dispersion equations with periodic boundary conditions. By the aid of the Fourier method, a procedure in Matlab is used to get the time step restriction of the schemes. For the convection-diffusion equations, the result shows that the IMEX finite difference schemes are stable under the condition $\Delta t \leq \max\{\tau_0, c\Delta x\}$, in which τ_0 is a positive constant proportional to the

TABLE 20. *The error and order for the schemes* (6), (25) *and* (26) *solving the equation* (30). *The time step is* $\Delta t = 0.1\Delta x$.

N	Norm	IMEX Runge-Kutta		Additive Runge-Kutta		multistep IMEX	
		error	order	error	order	error	order
160	L^1	5.36E-04		5.36E-04		6.40E-04	
	L^∞	1.29E-02		1.29E-02		1.88E-02	
320	L^1	9.18E-05	2.55	9.18E-05	2.55	1.15E-04	2.48
	L^∞	2.00E-03	2.68	2.00E-03	2.68	3.70E-03	2.34
640	L^1	1.27E-05	2.85	1.27E-05	2.85	2.28E-05	2.33
	L^∞	2.65E-04	2.92	2.65E-04	2.92	6.75E-04	2.46
1280	L^1	1.64E-06	2.96	1.64E-06	2.95	4.96E-06	2.20
	L^∞	3.35E-05	2.99	3.35E-05	2.99	1.18E-04	2.51
2560	L^1	2.07E-07	2.99	2.07E-07	2.99	1.23E-06	2.01
	L^∞	4.20E-06	3.00	4.20E-06	3.00	2.63E-05	2.17

diffusion coefficient and c is the Courant number. For the convection-dispersion equations, the result shows that the IMEX finite difference schemes are stable under the standard CFL condition $\Delta t \leq c\Delta x$. In addition, we can find that the Runge-Kutta type IMEX finite difference schemes admit larger time step than the multistep type IMEX finite difference schemes. The numerical tests verify the designed order of accuracy for these IMEX finite difference schemes under the stability condition.

Acknowledgments

References

[1] U. M. Ascher, S. J. Ruuth and B. T. R. Wetton, Implicit-explicit methods for time-dependent partial differential equations, SIAM Journal on Numerical Analysis, 32, 1995, 797-823.

[2] U. M. Ascher, S. J. Ruuth and R. J. Spiteri, Implicit-explicit Runge-Kutta methods for time-dependent partial differential equations, Applied Numerical Mathematics, 25, 1997, 151-167.

[3] J. Bruder, Linearly-implicit Runge-Kutta methods based on implicit Runge-Kutta methods, Applied Numerical Mathematics, 13, 1993, 33-40.

[4] M. P. Calvo, J. D. Frutos and J. Novo, Linearly implicit Runge-Kutta methods for advection-reaction-diffusion equations, Applied Numerical Mathematics, 37, 2001, 535-549.

[5] D. Dutykh, T. Katsaounis and D. Mitsotakis, Finite volume methods for unidirectional dispersive wave models, International Journal for Numerical Methods in Fluids, 71, 2013, 717-736.

[6] B. Fornberg and T. A. Driscoll, A fast spectral algorithm for nonlinear wave equations with linear dispersion, Journal of Computational Physics, 155, 1999, 456-467.

[7] J. Frank, W. Hundsdorfer and J. G. Verwer, On the stability of implicit-explicit linear multistep methods, Applied Numerical Mathematics, 25, 1997, 193-205.

[8] S. Gottlieb, C.-W. Shu and E. Tadmor, Strong stability-preserving high-order time discretization methods, SIAM Review, 43, 2001, 89-112.

[9] S. Gottlieb and C. Wang, Stability and convergence analysis of fully discrete Fourier collocation spectral method for 3-D viscous Burgers' equation, Journal of Scientific Computing, 53, 2012, 102-128.

[10] R. Guo and Y. Xu, Fast solver for the local discontinuous Galerkin discretization of the KdV type equations, Journal of Scientific Computing, 58, 2014, 380-408.

[11] A. C. Hindmarsh, P. M. Gresho and D. F. Griffiths, The stability of explicit Euler time-integration for certain finite difference approximations of the multi-dimensional advection-diffusion equation, International Journal for Numerical Methods in Fluids, 4, 1984, 853-897.

[12] G. S. Jiang and C.-W. Shu, Efficient implementation of weighted ENO schemes, Journal of Computational Physics, 126, 1996, 202-228.

[13] C. A. Kennedy and M. H. Carpenter, Additive Runge-Kutta schemes for convection-diffusion-reaction equations, Applied Numerical Mathematics, 44, 2003, 139-181.

[14] X. D. Liu, S. Osher and T. Chan, Weighted essentially non-oscillatory scheme, Journal of Computational Physics, 115, 1994, 200-212.

[15] C.-W. Shu, Essentially non-oscillatory and weighted essentially non-oscillatory schemes for hyperbolic conservation laws, in Advanced Numerical Approximation of Nonlinear Hyperbolic Equations, B. Cockburn, C. Johnson, C.-W. Shu and E. Tadmor (Editor: A. Quarteroni), Lecture Notes in Mathematics, volume 1697, Springer, Berlin, 1998, pp.325-432.

[16] H. J. Wang, C.-W. Shu and Q. Zhang, Stability and error estimates of local discontinuous Galerkin methods with implicit-explicit time-marching for advection-diffusion problems, SIAM Journal on Numerical Analysis, 53, 2015, 206-227.

[17] H. J. Wang, C.-W. Shu and Q. Zhang, Stability analysis and error estimates of local discontinuous Galerkin methods with implicit-explicit time-marching for nonlinear convection-diffusion problems, Applied Mathematics and Computation, 272, 2016, 237-258.

[18] H. J. Wang, Q. Zhang and C.-W. Shu, Implicit-explicit local discontinuous Galerkin methods with generalized alternating numerical fluxes convection-diffusion problems, Journal of Scientific Computing, 81, 2019, 1-35.

[19] J. Yan and C.-W. Shu, A local discontinuous Galerkin method for KdV type equations, SIAM Journal on Numerical Analysis, 40, 2002, 769-791.

[20] J. Zhu and C.-W. Shu, A new type of multi-resolution WENO schemes with increasingly higher order of accuracy, Journal of Computational Physics, 375, 2018, 659-683.

Appendix A

1. **The amplification factor G of the third order IMEX Runge-Kutta finite difference scheme** (5) **solving the convection-diffusion equation.**

Substituting the Fourier modes $u_j^n = v^n e^{Ikx_j}$, $I^2 = -1$ into the first four difference equations in (5) yields

$$v^{(2)} = \boldsymbol{M_2} v^n, \quad v^{(3)} = \boldsymbol{M_3} v^n, \quad v^{(4)} = \boldsymbol{M_4} v^n,$$

where

$$\boldsymbol{M_2} = \frac{1 + \Delta t \boldsymbol{GN}\hat{a}_{21}}{1 - \Delta t \boldsymbol{GL} a_{22}},$$

$$\boldsymbol{M_3} = \frac{1 + \Delta t \boldsymbol{GN}\big(\hat{a}_{31} + \hat{a}_{32}\boldsymbol{M_2}\big) + \Delta t \boldsymbol{GL} a_{32}\boldsymbol{M_2}}{1 - \Delta t \boldsymbol{GL} a_{33}},$$

$$\boldsymbol{M_4} = \frac{1 + \Delta t \boldsymbol{GN}\big(\hat{a}_{41} + \hat{a}_{42}\boldsymbol{M_2} + \hat{a}_{43}\boldsymbol{M_3}\big) + \Delta t \boldsymbol{GL}\big(a_{42}\boldsymbol{M_2} + a_{43}\boldsymbol{M_3}\big)}{1 - \Delta t \boldsymbol{GL} a_{44}},$$

$$\boldsymbol{GL} = -\frac{d}{12\Delta x^2}\Big(-32\cos\xi + 2\cos 2\xi + 30\Big),$$

$$\boldsymbol{GN} = -\frac{1}{\Delta x}\Big(\frac{1}{2} + \frac{1}{3}\cos\xi + \frac{1}{3}I\sin\xi - \cos\xi + I\sin\xi + \frac{1}{6}\cos 2\xi - \frac{1}{6}I\sin 2\xi\Big),$$

with ξ given by $\xi = k\Delta x$. The Butcher coefficients $a_{sj}, \hat{a}_{sj}, b_j, \hat{b}_j, s = 1,...,4; j = 1,...,4$ are specified in (6). Substitute the above formula into the last term of (5), and we can get the amplification factor G after a simple arithmetic operation.

$$G = 1 + \Delta t \boldsymbol{GN}\big(\hat{b}_1 + \hat{b}_2\boldsymbol{M_2} + \hat{b}_3\boldsymbol{M_3} + \hat{b}_4\boldsymbol{M_4}\big) + \Delta t \boldsymbol{GL}\big(b_2\boldsymbol{M_2} + b_3\boldsymbol{M_3} + b_4\boldsymbol{M_4}\big).$$

2. **The coefficients of the characteristic equation** (16).

$$a_1 = \frac{1 + \frac{23}{12}\Delta t \boldsymbol{GN}}{1 - \frac{2}{3}\Delta t \boldsymbol{GL}}, \quad a_2 = \frac{-\frac{4}{3}\Delta t \boldsymbol{GN} + \frac{5}{12}\Delta t \boldsymbol{GL}}{1 - \frac{2}{3}\Delta t \boldsymbol{GL}},$$

$$a_3 = \frac{\frac{5}{12}\Delta t \boldsymbol{GN}}{1 - \frac{2}{3}\Delta t \boldsymbol{GL}}, \qquad a_4 = \frac{-\frac{1}{12}\Delta t \boldsymbol{GL}}{1 - \frac{2}{3}\Delta t \boldsymbol{GL}}.$$

Appendix B

For the IMEX Runge-Kutta finite difference scheme (5), the Courant number c and the maximum time step τ_0 have been obtained numerically using the Matlab code. Note that the stability analysis described in Section 2.1.1 is carried out by considering whether the condition $|G| \leq 1$ is satisfied. Taking the maximum time step τ_0 as an example, the algorithm developed for the scheme is presented below.

Algorithm 1 : Numerical stability analysis of the third order IMEX Runge-Kutta finite difference scheme (5) for solving the linear convection-diffusion equation with periodic boundary condition.

Require: d: diffusion coefficient
Ensure: τ_0: the maximum time step
1: **function** MAINFUNCTION(d)
2: $\tau_0 \leftarrow 0$
3: $bool_1 \leftarrow 1$
4: $N \leftarrow 10^5$
5: $\Delta x \leftarrow \frac{\pi}{N}$
6: **while** (1) **do**
7:    $\Delta t \leftarrow \tau_0$
8:    **for** $k = -N + 1 \to N$ **do**
9:      compute $|G|$, where G is a function of $d, \Delta t, \Delta x, k$
10:      **if** $|G| > 1$ **then**
11:        $bool_1 \leftarrow 0$
12:        break;
13:      **end if**
14:    **end for**
15:    **if** $bool_1 \neq 0$ **then**
16:      $\tau_0 \leftarrow \tau_0 + 0.01$
17:    **else**
18:      break;
19:    **end if**
20: **end while**
21: **return** τ_0
22: **end function**

Graduate School, China Academy of Engineering Physics, Beijing 100088, China.
E-mail: `tanmeiqi20@gscaep.ac.cn.`

Laboratory of Computational Physics, Institute of Applied Physics and Computational Mathematics, Beijing 100088, China and Center for Applied Physics and Technology, Peking University, Beijing 100871, China.
E-mail: `cheng_juan@iapcm.ac.cn.`

Division of Applied Mathematics, Brown University, Providence, RI 02912.
E-mail: `chi-wang_shu@brown.edu.`